PHYSICAL REVIEW D **93,** 116008 (2016)

Localized direct CP violation for $B^{\pm} \to \rho^0(\omega)\pi^{\pm} \to \pi^+\pi^-\pi^{\pm}$ in QCD factorization

Chao Wang,[1,3,†] Zhen-Yang Wang,[1,‡] Zhen-Hua Zhang,[2,§] and Xin-Heng Guo[1,*]

[1]*College of Nuclear Science and Technology, Beijing Normal University, Beijing 100875, China*
[2]*School of Nuclear Science and Technology, University of South China, Hengyang 421001, Hunan, China*
[3]*Center for Ecological and Environmental Sciences, Northwestern Polytechnical University, Xi'an 710072, Shaanxi, China*

(Received 11 February 2016; revised manuscript received 14 June 2016; published 30 June 2016)

We study the localized direct CP violation in the hadronic decays $B^{\pm} \to \rho^0(\omega)\pi^{\pm} \to \pi^+\pi^-\pi^{\pm}$, including the effect caused by an interesting mechanism involving the charge symmetry violating mixing between ρ^0 and ω in the QCD factorization approach. We find that ρ-ω mixing makes the localized integrated CP asymmetry move toward the negative direction when the low invariant mass of $\pi^+\pi^-$ [$m(\pi^+\pi^-)_{\mathrm{low}}$] is near $\rho^0(770)$. The localized integrated direct CP violation obtained in the QCD factorization approach varies from -0.0724 to -0.0389 in the ranges of parameters when $0.750 < m(\pi^+\pi^-)_{\mathrm{low}} < 0.800$ GeV. This result, especially the sign, agrees with the experimental data. We also calculate the localized integrated direct CP violating asymmetries in the QCD factorization approach in the regions $0.470 < m(\pi^+\pi^-)_{\mathrm{low}} < 0.770$ GeV and $0.770 < m(\pi^+\pi^-)_{\mathrm{low}} < 0.920$ GeV. We find that these results agree with the experimental data and are more accurate than the results obtained through the naive factorization approach. It is more clear that ρ-ω mixing contributes to the sign change in these two regions.

DOI: 10.1103/PhysRevD.93.116008

I. INTRODUCTION

CP violation is one of the most fundamental and important properties of weak interactions. Even though it has been known since 1964 [1], we still do not know the source of CP violation completely. In the standard model, CP violation is originated from the weak phase in the Cabibbo-Kobayashi-Maskawa (CKM) matrix [2,3]. Besides the weak phase, a large strong phase is also needed for direct CP violation to occur in decay processes. Usually, this large phase is provided by QCD loop corrections and some phenomenological mechanisms.

It was suggested long time ago that large CP violation should be observed in the B meson systems [4,5]. In the past few years, more attention has been focused on CP violations in the B and D meson systems both theoretically and experimentally. Recently, the LHCb Collaboration has focused on three-body final states in the decays of B and D mesons and a novel strategy to probe CP asymmetries in their Dalitz plots [6–8]. The local asymmetries in specific regions of the phase space of charmless three-body decays of bottom mesons, such as $B^{\pm} \to \pi^{\pm}\pi^+\pi^-$ and $B^{\pm} \to K^{\pm}\pi^+\pi^-$, were measured. It was shown that the local asymmetry distributions in the Dalitz plots reveal rich structures and are not uniform [6–8]. These intriguing discoveries offer opportunities to search for different sources of CP violation through the study of the signatures of these sources in certain phase spaces of the Dalitz plots. It was claimed that the CP asymmetry in these decays changes sign around the $\rho^0(770)$ peak in the $B^{\pm} \to \pi^{\pm}\pi^+\pi^-$ decays [8]. The experimental values of the localized integrated CP asymmetries in the regions $0.470 < m(\pi^+\pi^-)_{\mathrm{low}} < 0.770$ GeV and $0.770 < m(\pi^+\pi^-)_{\mathrm{low}} < 0.920$ GeV are 0.0508 ± 0.0171 and -0.0256 ± 0.0202, respectively, with opposite signs [8].

In our previous work, we noted that ρ-ω mixing contributes to the sign change around the $\rho^0(770)$ peak [9]. ρ-ω mixing is an interesting phenomenological mechanism involving the charge symmetry violating mixing between ρ^0 and ω. This mechanism was considered to obtain a large strong phase and lead to a peak of CP violation when the invariant mass of $\pi^+\pi^-$ is near ω in B and τ decays [10–13]. The differential CP asymmetry was studied in the decays $B^{\pm} \to \rho^0(\omega)\pi^{\pm} \to \pi^+\pi^-\pi^{\pm}$ in the naive factorization, QCD factorization and perturbative QCD approaches, respectively [14–16]. We calculated localized integrated direct CP violation involving ρ-ω mixing and discussed the sign change caused by such mixing working in the naive factorization approach [9]. In the calculations, the nonfactorizable contribution is effectively absorbed into a color parameter which is extracted from data of branching ratios. The B meson decay amplitude involves the hadronic matrix element which computation is nontrivial. For the two-body nonleptonic decay process of the bottom hadron, the naive factorization approach appears as the leading order result of the QCD

*Corresponding author.
xhguo@bnu.edu.cn
†chaowang11@mail.bnu.edu.cn
‡rongtian@mail.bnu.edu.cn
§zhangzh@usc.edu.cn

factorization scheme with the $1/m_b$ and $\alpha_s(m_b)$ corrections being neglected [17,18]. For the calculation of decay branching ratios, the naive factorization approximation is expected to be a good method. But for the much more subtle calculation of direct CP violation, different approaches may produce different strong phases [16–21]. The strong phase is usually difficult to control and depends sensitively on the calculation method. In the naive factorization approach, the strong phase is introduced phenomenologically via the effective Wilson coefficients [9,14]. In the QCD factorization approach, the strong phase can be generated dynamically, which is more reliable [17,18]. Therefore, in the present work we will calculate the localized integrated CP asymmetry in the decays $B^\pm \to \pi^\pm\pi^+\pi^-$ involving ρ-ω mixing in the QCD factorization approach, which is a more modern method, and compare the results with those from the naive factorization approach.

We will see that our result for the localized integrated CP asymmetry varies from -0.0724 to -0.0389, which is more accurate than those from the naive factorization approach when $0.750 < m(\pi^+\pi^-)_{\rm low} < 0.800$ GeV. This result still agrees with the experimental data. As for the regions $0.470 < m(\pi^+\pi^-)_{\rm low} < 0.770$ GeV and $0.770 < m(\pi^+\pi^-)_{\rm low} < 0.920$ GeV, the localized integrated CP violations obtained in the QCD factorization approach also agree with the experimental data and are more accurate comparing with those obtained in the naive factorization approach. We will see clearly that ρ-ω mixing makes the localized integrated CP asymmetries move toward the negative direction and therefore contributes to the sign change between the regions $0.470 < m(\pi^+\pi^-)_{\rm low} < 0.770$ GeV and $0.770 < m(\pi^+\pi^-)_{\rm low} < 0.920$ GeV.

The remainder of this paper is organized as follows. In Sec. II, we present the form of the effective Hamiltonian and review the QCD factorization formalism briefly. Then, we show the formalism for the CP violating asymmetry in $B^\pm \to \rho^0(\omega)\pi^\pm \to \pi^+\pi^-\pi^\pm$ in Sec. III. In Sec. IV we give the input parameters and show numerical results. We also compare the results obtained in the QCD factorization and naive factorization approaches in this section. In the last section, we give some discussions and summarize our results.

II. QCD FACTORIZATION

The effective Hamiltonian in bottom hadron decays based on the operator product expansion is [17]

$$\mathcal{H} = \frac{G_F}{\sqrt{2}}\left[\sum_{p=u,c}\sum_{D=d,s}\lambda_p^{(D)}\left(c_1 O_1^p + c_2 O_2^p + \sum_{i=3}^{10} c_i O_i\right)\right] + \mathrm{H.c.}, \tag{1}$$

where $\lambda_p^{(D)} = V_{pb}V_{pD}^*$, c_i $(i = 1, \ldots, 10, 7\gamma, 8g)$ are the Wilson coefficients, which are calculable in the renormalization group improved perturbation theory and are scale dependent, V_{pb} and V_{pq} are the CKM matrix elements. In the present work, we use the values of the Wilson coefficients at the renormalization scale $\mu \approx m_b$ [17,18]. The operators O_i have the following forms:

$$\begin{aligned}
&O_1^p = \bar{p}\gamma_\mu(1-\gamma_5)b\bar{D}\gamma^\mu(1-\gamma_5)p, && O_2^p = \bar{p}_\alpha\gamma_\mu(1-\gamma_5)b_\beta\bar{D}_\beta\gamma^\mu(1-\gamma_5)p_\alpha,\\
&O_3 = \bar{D}\gamma_\mu(1-\gamma_5)b\sum_{q'}\bar{q}'\gamma^\mu(1-\gamma_5)q', && O_4 = \bar{D}_\alpha\gamma_\mu(1-\gamma_5)b_\beta\sum_{q'}\bar{q}'_\beta\gamma^\mu(1-\gamma_5)q'_\alpha,\\
&O_5 = \bar{D}\gamma_\mu(1-\gamma_5)b\sum_{q'}\bar{q}'\gamma^\mu(1+\gamma_5)q', && O_6 = \bar{D}_\alpha\gamma_\mu(1-\gamma_5)b_\beta\sum_{q'}\bar{q}'_\beta\gamma^\mu(1+\gamma_5)q'_\alpha,\\
&O_7 = \tfrac{3}{2}\bar{D}\gamma_\mu(1-\gamma_5)b\sum_{q'}e_{q'}\bar{q}'\gamma^\mu(1+\gamma_5)q', && O_8 = \tfrac{3}{2}\bar{D}_\alpha\gamma_\mu(1-\gamma_5)b_\beta\sum_{q'}e_{q'}\bar{q}'_\beta\gamma^\mu(1+\gamma_5)q'_\alpha,\\
&O_9 = \tfrac{3}{2}\bar{D}\gamma_\mu(1-\gamma_5)b\sum_{q'}e_{q'}\bar{q}'\gamma^\mu(1-\gamma_5)q', && O_{10} = \tfrac{3}{2}\bar{D}_\alpha\gamma_\mu(1-\gamma_5)b_\beta\sum_{q'}e_{q'}\bar{q}'_\beta\gamma^\mu(1-\gamma_5)q'_\alpha,\\
&O_{7\gamma} = \tfrac{-e}{8\pi^2}m_b\bar{s}\sigma_{\mu\nu}(1+\gamma_5)F^{\mu\nu}b, && O_{8g} = \tfrac{-g_s}{8\pi^2}m_b\bar{s}\sigma_{\mu\nu}(1+\gamma_5)G^{\mu\nu}b,
\end{aligned} \tag{2}$$

where α and β are color indices, $q' = u, d, s, c$ or b quarks. In Eq. (2), O_1^p and O_2^p are the tree level operators, $O_3 - O_6$ are QCD penguin operators, $O_7 - O_{10}$ arise from electroweak penguin diagrams, and $O_{7\gamma}$ and O_{8g} are the electromagnetic and chromomagnetic dipole operators, respectively.

In QCD factorization, we consider the weak decay $B \to M_1M_2$ (M_i refers to ρ^0, ω or π^- in our calculations) in the heavy-quark limit. In this limit, the transition matrix element of an operator O_i in the weak effective Hamiltonian is given by [17]

$$\begin{aligned}
\langle M_1M_2|O_i|B\rangle = {}& \sum_j F_j^{B\to M_1}(m_2^2)\int_0^1 \mathrm{d}u T_{ij}^I(u)\Phi_{M_2}(u) + (M_1 \leftrightarrow M_2)\\
&+ \int_0^1 \mathrm{d}\xi \mathrm{d}u \mathrm{d}v T_i^{II}(\xi, u, v)\Phi_B(\xi)\Phi_{M_1}(v)\Phi_{M_2}(u),
\end{aligned} \tag{3}$$

where $F_j^{B\to M_{1,2}}(m_{2,1}^2)$ denotes a $B\to M_{1,2}$ form factor with $m_{1,2}$ being the mass of the light meson $M_{1(2)}$, $\Phi_{M_{1(2)}}(x)$ and $\Phi_{m_{1(2)}}(x)$ are the leading-twist and twist-3 light cone distribution amplitudes (LCDA), respectively, with x being the light-cone momentum fraction of the quark inside the meson, and $T_{ij}^{I}(u)$ and $T_i^{II}(\xi,u,v)$ are hard scattering kernels, which are calculated order by order in perturbation theory. The vertex and penguin corrections are included at the order of α_s in T_{ij}^I. The hard interactions [at order $\mathcal{O}(\alpha_s)$] between the spectator quark and the emitted meson, at large gluon momentum, are taken into account by T_i^{II}.

The matrix element is given by [17]

$$\langle M_1M_2|\mathcal{H}|B\rangle=\sum_{p=u,c}\lambda_p^{(D)}\langle M_1M_2|\mathcal{T}_A^p+\mathcal{T}_B^p|B\rangle, \tag{4}$$

where the two terms account for the flavor topologies of the form factor and hard scattering terms in Eq. (3), respectively.

The expression of $\mathcal{T}_A^p$ is

$$\begin{aligned}\mathcal{T}_A^p&=\delta_{pu}\alpha_1^p(M_1M_2)A([\bar q_s u][\bar u D])+\delta_{pu}\alpha_2^p(M_1M_2)A([\bar q_s D][\bar u u])\\&\quad+\alpha_3^p(M_1M_2)\sum_q A([\bar q_s D][\bar q q])+\alpha_4^p(M_1M_2)\sum_q A([\bar q_s q][\bar q D])\\&\quad+\alpha_{3,\mathrm{EW}}^p(M_1M_2)\sum_q\frac{3}{2}e_qA([\bar q_s D][\bar q q])+\alpha_{4,\mathrm{EW}}^p(M_1M_2)\sum_q\frac{3}{2}e_qA([\bar q_s q][\bar q D]),\end{aligned} \tag{5}$$

where the sums extend over $q=u$, d, s, and $\bar q_s$ ($=u$, d, or s) denotes the spectator antiquark. The symbol $A([\cdots][\cdots])$ indicates that the matrix elements of the operators in $\mathcal{T}_A^p$ are to be evaluated in the factorized form, such as $\langle M_1M_2|A([\bar q_s u][\bar u D])|B\rangle=\langle M_1|[\bar q_s u]|0\rangle\langle M_2|[\bar u D]|B\rangle$, where the quark flavors of the first (second) square bracket match those of M_1 (M_2). The coefficients $\alpha_i^p(M_1M_2)$ and $\alpha_{i,\mathrm{EW}}^p(M_1M_2)$ contain all dynamical information and can be expressed in terms of the coefficients a_i^p defined in Ref. [17]. The general form of the coefficients $a_i^p(M_1M_2)$ at the next-to-leading order in α_s is [17]

$$a_i^p(M_1M_2)=\left(c_i+\frac{c_{i\pm1}}{N_c}\right)N_i(M_2)+\frac{c_{i\pm1}}{N_c}\frac{C_F\alpha_s}{4\pi}\left[V_i(M_2)+\frac{4\pi^2}{N_c}H_i(M_1M_2)\right]+P_i^p(M_2), \tag{6}$$

where $N_i(M_2)=0$ if $i=6$, 8 with $M_2=V$, and $N_i(M_2)=1$ for all other cases [$V(P)$ denotes a vector (pseudoscalar) meson]. The first two terms in Eq. (6) include the results of the naive factorization followed by the vertex, the hard-spectator, and the penguin corrections, which formulas can be found in Refs. [17,18]. As stressed in Refs. [17,18], the hard-spectator interactions and penguin corrections should be evaluated at the hard-collinear scale $\mu_h=\sqrt{\Lambda_h\mu}$ with $\Lambda_h=0.5$ GeV.

$\mathcal{T}_B^p$ includes the power-suppressed annihilation parts and can be parametrized in its most general form as

$$\begin{aligned}\mathcal{T}_B^p&=\delta_{pu}b_1(M_1M_2)\sum_{q''}B([\bar u q''][\bar q'' u][\bar D b])+\delta_{pu}b_2(M_1M_2)\sum_{q''}B([\bar u q''][\bar q'' D][\bar u b]))\\&\quad+b_{3,\mathrm{EW}}(M_1M_2)\sum_{q,q''}\frac{3}{2}e_qB([\bar q q''][\bar q' D][\bar q b])+b_{4,\mathrm{EW}}(M_1M_2)\sum_{q,q''}\frac{3}{2}e_qB([\bar q q''][\bar q'' q][\bar D b])\\&\quad+b_3(M_1M_2)\sum_{q,q''}B([\bar q q''][\bar q'' D][\bar q b])+b_4(M_1M_2)\sum_{q,q''}B([\bar q q''][\bar q'' q][\bar D b]),\end{aligned} \tag{7}$$

where the sums extend over q, $q''=u$, d, s. The sum over q'' arises because a quark-antiquark pair must be created via $g\to\bar q'' q''$ after the spectator quark is annihilated. We define the matrix elements of a operator $B([\cdots][\cdots][\cdots])$ as in Refs. [17,18]

$$\langle M_1M_2|B([\cdots][\cdots][\cdots])|B\rangle\equiv \mathrm{i}G_Ff_Bf_{M_1}f_{M_2}, \tag{8}$$

where the quark flavors of the three brackets match those of M_1, M_2 and B and f_X ($X=B,\rho^0,\omega$ or π) is the decay constant of X.

The coefficients b_i in Eq. (7) are expressed in the following forms [17]:

$$\begin{aligned} b_1 &= \frac{C_F}{N_c^2} c_1 A_1^i, \qquad b_2 = \frac{C_F}{N_c^2} c_2 A_1^i, \\ b_3 &= \frac{C_F}{N_c^2} \{ c_3 A_1^i + c_5 A_3^i + [c_5 + N_c c_6] A_3^f \}, \\ b_{3,\mathrm{EW}} &= \frac{C_F}{N_c^2} \{ c_9 A_1^i + c_7 A_3^i + [c_7 + N_c c_8] A_3^f \}, \\ b_4 &= \frac{C_F}{N_c^2} \{ c_4 A_1^i + c_6 A_2^i \}, \\ b_{4,\mathrm{EW}} &= \frac{C_F}{N_c^2} \{ c_{10} A_1^i + c_8 A_2^i \}, \end{aligned} \tag{9}$$

where $A_k^{i(f)}(M_1 M_2)$ ($\equiv A_k^{i(f)}$ for simplicity) are obtained in terms of convolutions of hard scattering kernels with the light cone expansions and the superscript i (f) refers to gluon emission from the initial (final) state quarks. The expressions of $A_k^{i(f)}(M_1 M_2)$ can be found in Ref. [17].

The calculations of the hard-spectator interaction corrections involve the twist-3 distribution amplitude. It happens that these contributions involve endpoint divergences because of the nonvanishing endpoint behavior of Φ_{m_i} [17,18]. We extract this divergence by defining a parameter $X_H^{M_i}$ through [17,18]

$$\begin{aligned} \int_0^1 \frac{\mathrm{d}x}{\bar{x}} \Phi_{m_i}(x) &= \Phi_{m_i}(1) \int_0^1 \frac{\mathrm{d}x}{\bar{x}} + \int_0^1 \frac{\mathrm{d}x}{\bar{x}} [\Phi_{m_1}(x) - \Phi_{m_i}(1)] \\ &\equiv \Phi_{m_i}(1) X_H^{M_1} + \int_0^1 \frac{\mathrm{d}x}{[\bar{x}]_+} \Phi_{m_i}(x) \end{aligned} \tag{10}$$

with $\bar{x} \equiv 1 - x$. The remaining integral is finite (it vanishes for pseudoscalar mesons), but $X_H^{M_i}$ is an unknown parameter representing soft-gluon interaction with the spectator quark. The annihilation corrections also exhibit endpoint divergences which can be treated in the same manner as the hard-spectator interactions and interpreted as [17,18]

$$\int_0^1 \frac{\mathrm{d}x}{x} \to X_A^{M_i}, \qquad \int_0^1 \mathrm{d}x \frac{\ln x}{x} \to -\frac{1}{2} (X_A^{M_i})^2. \tag{11}$$

We assume that the divergence parameters for the hard-spectator interaction and the annihilation correction are universal [17,18]. However, for the $B \to VP$ and $B \to PV$ decays, the divergence parameters (X^{PV} and X^{VP}) are not necessarily the same [22]. In the calculations, we parametrize the divergence integrals by [17,18]:

$$X^{PV(VP)} = (1 + \rho^{PV(VP)} e^{\mathrm{i}\phi^{PV(VP)}}) \ln \frac{m_B}{\Lambda_h}, \tag{12}$$

where $\rho^{PV(VP)}$ and $\phi^{PV(VP)}$ are real parameters which will be given in the following.

III. *CP* VIOLATION IN $B^\pm \to \rho^0(\omega)\pi^\pm \to \pi^+\pi^-\pi^\pm$

A. Formalism for *CP* violation

The amplitude for the decay $B^- \to \pi^+\pi^-\pi^-$ through the vector resonance (ρ^0 and ω) can be expressed as [9,14,23–25]:

$$A = (\Sigma - s')\mathcal{M} = \langle \pi^+\pi^-\pi^- | \mathcal{H}^T | B^- \rangle + \langle \pi^+\pi^-\pi^- | \mathcal{H}^P | B^- \rangle, \tag{13}$$

where $\mathcal{H}^T$ and $\mathcal{H}^P$ are the Hamiltonians for the tree and penguin operators, respectively, $\sqrt{s'}$ is the high invariance mass of the $\pi^+\pi^-$ pair, $\Sigma = \frac{1}{2}(s'_{\mathrm{max}} + s'_{\mathrm{min}})$ with s'_{max} and s'_{min} being the maximum and minimum values of s' for a fixed s, respectively, and $\sqrt{s}$ is the low invariant mass of the $\pi^+\pi^-$ pair $[m(\pi^+\pi^-)_{\mathrm{low}}]$. In order to obtain a large signal for direct *CP* violation, we need to appeal to some phenomenological mechanisms. ρ-ω mixing has the dual advantages that the strong phase difference is large (passes through 90° at the ω resonance) and well known [11,12]. With this mechanism, to the first order in isospin violation, the amplitude for $B^- \to \rho^0(\omega)\pi^- \to \pi^+\pi^-\pi^-$ takes the following form at a value of $\sqrt{s}$ close to the ω resonance mass [14]:

$$\langle \pi^+\pi^-\pi^- | \mathcal{H}^T | B^- \rangle = (\Sigma - s') \left(\frac{g_\rho}{s_\rho s_\omega} \tilde{\Pi}_{\rho\omega} t_\omega + \frac{g_\rho}{s_\rho} t_\rho \right), \tag{14}$$

$$\langle \pi^+\pi^-\pi^- | \mathcal{H}^P | B^- \rangle = (\Sigma - s') \left(\frac{g_\rho}{s_\rho s_\omega} \tilde{\Pi}_{\rho\omega} p_\omega + \frac{g_\rho}{s_\rho} p_\rho \right), \tag{15}$$

where t_V ($V = \rho^0$ or ω) is the tree amplitude and p_V is the penguin amplitude for producing an intermediate vector meson V, g_ρ is the coupling for $\rho^0 \to \pi^+\pi^-$, $\tilde{\Pi}_{\rho\omega}$ is the effective ρ-ω mixing amplitude, and s_V is from the inverse propagator of the vector meson V, $s_V = s - m_V^2 + \mathrm{i} m_V \Gamma_V$.

From Eqs. (14) and (15), we note that ρ-ω mixing provides an additional complex term for the tree and penguin amplitudes (the first term in each equation), respectively. These complex terms will enlarge the *CP*-even phase, and lead to a peak of *CP* asymmetry as mentioned before. We will show the difference between the *CP* asymmetries with and without ρ-ω mixing later. Here, we assume that the $B^\pm \to \pi^+\pi^-\pi^\pm$ process is dominated by the resonance ρ^0 in a certain region of its Dalitz plot.

We stress that the direct coupling $\omega \to \pi^+\pi^-$ is effectively absorbed into $\tilde{\Pi}_{\rho\omega}$ [26], leading to the explicit s dependence of $\tilde{\Pi}_{\rho\omega}$. Making the expansion $\tilde{\Pi}_{\rho\omega}(s) = \tilde{\Pi}_{\rho\omega}(m_\omega^2) + (s - m_\omega^2)\tilde{\Pi}'_{\rho\omega}(m_\omega^2)$, the ρ-ω mixing parameters were determined in the fit of Gardner and O'Connell [27]: $\mathfrak{Re}\tilde{\Pi}_{\rho\omega}(m_\omega^2) = -3500 \pm 300\ \mathrm{MeV}^2$,

$\mathfrak{Im}\tilde{\Pi}_{\rho\omega}(m_\omega^2) = -300 \pm 300\,\mathrm{MeV}^2$, $\tilde{\Pi}'_{\rho\omega}(m_\omega^2) = 0.03 \pm 0.04$. In practice, the effect of the derivative term is negligible.

In this work, we only consider ρ^0 and ω resonances. Then, for a fixed s, the differential CP asymmetry parameter can be defined as

$$A_{CP} = \frac{|\mathcal{M}|^2 - |\bar{\mathcal{M}}|^2}{|\mathcal{M}|^2 + |\bar{\mathcal{M}}|^2}. \tag{16}$$

By integrating the denominator and numerator of A_{CP}, respectively, in the region Ω ($s_1 < s < s_2$, $s'_1 < s' < s'_2$), we obtain the localized integrated CP asymmetry, which can be measured by experiments and takes the following form:

$$A_{CP}^{\Omega} = \frac{\int_{s_1}^{s_2} \mathrm{d}s \int_{s'_1}^{s'_2} \mathrm{d}s' (\Sigma - s')^2 (|\mathcal{M}|^2 - |\bar{\mathcal{M}}|^2)}{\int_{s_1}^{s_2} \mathrm{d}s \int_{s'_1}^{s'_2} \mathrm{d}s' (\Sigma - s')^2 (|\mathcal{M}|^2 + |\bar{\mathcal{M}}|^2)}. \tag{17}$$

According to kinematics of the three body decay, $\Sigma[= \frac{1}{2}(s'_{\max} + s'_{\min})]$ is related to s. In our calculations, s varies in a small region, and therefore Σ can be treated as a constant approximately [8]. Then, the terms $\int_{s'_1}^{s'_2} \mathrm{d}s' (\Sigma - s')^2$ are canceled, and A_{CP}^{Ω} becomes independent of the high invariant mass of $\pi^+\pi^-$. In practice, to be more precise, we take into account the s-dependence of $s'_{\max}$ and $s'_{\min}$ in our calculations. We choose $s'_{\min} < s' < s'_{\max}$ as the integration interval of the high invariance mass of $\pi^+\pi^-$ and regard $\int_{s'_{\min}}^{s'_{\max}} \mathrm{d}s' (\Sigma - s')^2$ as a factor which is dependent on s.

B. The tree and penguin amplitudes

With the Hamiltonian given in Eq. (1), we are ready to evaluate the matrix elements for $B^- \to \rho^0(\omega)\pi^-$ in QCD factorization. The matrix elements for $B \to P$ and $B \to V$ can be decomposed as [28]

$$\langle P|J_\mu|B\rangle = \left(p_B + p_P - \frac{m_B^2 - m_P^2}{k^2}\right)_\mu F_1^{BP}(k^2) + \frac{m_B^2 - m_P^2}{k^2} k_\mu F_0^{BP}(k^2), \tag{18}$$

$$\langle V|J_\mu|B\rangle = \frac{2}{m_B + m_V} \varepsilon_{\mu\nu\rho\sigma} \epsilon^{*\nu} p_B^\rho p_V^\sigma V^{BV}(k^2) + \mathrm{i}\left\{\epsilon_\mu^*(m_B + m_V) A_1^{BV}(k^2) - \frac{\epsilon^* \cdot k}{m_B + m_V}(p_B + p_V)_\mu A_2^{BV}(k^2) - \frac{\epsilon^* \cdot k}{k^2} 2m_V \cdot k_\mu A_3^{BV}(k^2)\right\} + \mathrm{i}\frac{\epsilon^* \cdot k}{k^2} 2m_V \cdot k_\mu A_0^{BV}(k^2), \tag{19}$$

where J_μ is the weak current [$J_\mu = \bar{u}\gamma_\mu(1-\gamma_5)b$ or $\bar{d}\gamma_\mu(1-\gamma_5)b$], k is the difference of momentum between B and $P(V)$, and ϵ_μ is the polarization vector of V, $F_i^{BP}(k^2)$ ($i = 0, 1$) and $A_i^{BV}(k^2)$ ($i = 0, 1, 2, 3$) are the weak form factors. The form factors included in our calculations satisfy $F_1^{BP}(0) = F_0^{BP}(0)$, $A_3^{BV}(0) = A_0^{BV}(0)$, and $A_3^{BV}(k^2) = [(m_B + m_V)/2m_V]A_1^{BV}(k^2) - [(m_B - m_V)/2m_V]A_2^{BV}(k^2)$.

Then, from Eqs. (5) and (7), we have

$$t_\rho = -\mathrm{i}G_F\lambda_u^{(D)}\{m_\rho f_\rho F_1^{B\pi}(m_\rho^2)\alpha_2^u(\pi\rho) + m_\rho f_\pi A_0^{B\rho}(m_\pi^2)\alpha_1^u(\rho\pi) + f_B f_\pi f_\rho[b_2(\rho\pi) - b_2(\pi\rho)]\}, \tag{20}$$

$$t_\omega = -\mathrm{i}G_F\lambda_u^{(D)}\{m_\omega f_\omega F_1^{B\pi}(m_\omega^2)\alpha_2^u(\pi\omega) + m_\omega f_\pi A_0^{B\omega}(m_\pi^2)\alpha_1^u(\omega\pi)] + f_B f_\pi f_\omega[b_2(\omega\pi) + b_2(\pi\omega)\}, \tag{21}$$

where the expressions for all the α_i and b_i have been given before. In the same way, we obtain the penguin operator contributions:

$$p_\rho = -\mathrm{i}G_F\sum_{p=u,c}\lambda_p^{(D)}\left\{m_\rho f_\pi A_0^{B\rho}(m_\pi^2)[\alpha_4^p(\rho\pi) + \alpha_{4,\mathrm{EW}}^p(\rho\pi)] + m_\rho f_\rho F_1^{B\pi}(m_\rho^2)\left[\alpha_{3,\mathrm{EW}}^p(\pi\rho) - \alpha_4^p(\pi\rho) + \frac{1}{2}\alpha_{4,\mathrm{EW}}^p(\pi\rho)\right] + f_B f_\pi f_\rho[b_3(\rho\pi) + b_{3,\mathrm{EW}}(\rho\pi) - b_3(\pi\rho) - b_{3,\mathrm{EW}}(\pi\rho)]\right\}, \tag{22}$$

$$p_\omega = -\mathrm{i}G_F\sum_{p=u,c}\lambda_p^{(D)}\left\{m_\omega f_\pi A_0^{B\omega}(m_\pi^2)[\alpha_{4,\mathrm{EW}}^p(\pi\omega) + \alpha_{4,\mathrm{EW}}^p(\omega\pi)] + m_\omega f_\omega F_1^{B\pi}(m_\omega^2)\left[2\alpha_3^p(\pi\omega) + \frac{1}{2}\alpha_{3,\mathrm{EW}}^p(\pi\omega) + \alpha_{4,\mathrm{EW}}^p(\pi\omega)\right] + f_B f_\pi f_\omega[b_3(\omega\pi) + b_{3,\mathrm{EW}}(\pi\omega) + b_3(\omega\pi) + b_{3,\mathrm{EW}}(\omega\pi)]\right\}. \tag{23}$$

IV. NUMERICAL RESULTS

A. Input parameters

The predictions obtained in the QCD factorization approach depend on many input parameters. In the QCD factorization approach, since power corrections have been considered, N_c is simply a color parameter and we use $N_c = 3$. The CKM matrix in the Wolfenstein parametrization can be determined from the experimental data. Since λ and A are well determined and the uncertainties due to the CKM matrix elements are mostly from ρ and η, we take the central values of λ $(= 0.225)$ and A $(= 0.814)$. We use the following values of ρ and η [29]:

$$\bar{\rho} = 0.117 \pm 0.021, \qquad \bar{\eta} = 0.353 \pm 0.013 \tag{24}$$

with

$$\bar{\rho} = \rho\left(1 - \frac{\lambda^2}{2}\right), \qquad \bar{\eta} = \eta\left(1 - \frac{\lambda^2}{2}\right). \tag{25}$$

The Wilson coefficients c_i at the renormalization scale $\mu = m_b$ can be found in Ref. [18].

The quark mass is taken at the scale $\mu = m_b$ in B decays (in MeV) [17,18]:

$$m_u = m_d = 3.7, \quad m_s = 90, \quad m_c = 1300, \quad m_b = 4200. \tag{26}$$

For meson masses, we shall use the following values (in MeV) [29]:

$$m_{B^\pm} = 5279, \quad m_{\pi^\pm} = 139, \quad m_\omega = 782, \quad m_\rho = 775.$$

The chiral enhancement factor $r_\chi^{M_i}$ for the pseudoscalar meson M_i is parametrized by the term $r_\chi^{M_i}(\mu) = \frac{2m_i^2}{m_b(\mu)(m_q+m_s)(\mu)}$ [17,18] where m_q denotes the average of the up and down quark masses. For the vector meson M_i, we have $r_\chi^{M_i}(\mu) = \frac{2m_i}{m_b(\mu)}\frac{f_{M_i}^\perp(\mu)}{f_{M_i}}$ [17,18] where the scale-dependent transverse decay constant $f_{M_2}^\perp$ is defined as $\langle M_2(p,\varepsilon^*)|\bar{q}\sigma_{\mu\nu}q'|0\rangle = f_{M_2}^\perp(p_\mu\varepsilon_\nu^* - p_\nu\varepsilon_\mu^*)$. For the decay constants we take (in MeV) [22]

$$\begin{aligned} &f_\pi = 131, \quad f_B = 210 \pm 20, \quad f_\rho = 216 \pm 3, \\ &f_\omega = 187 \pm 5, \quad f_\rho^\perp = 165 \pm 9, \quad f_\omega^\perp = 151 \pm 9, \end{aligned} \tag{27}$$

where $f_V^\perp$ is given for $\mu = 1$ GeV.

The LCDA Φ_{M_i} is the leading-twist amplitude of M_i, whereas Φ_{m_i} is the twist-3 amplitude. The leading-twist LCDA for the pseudoscalar and vector mesons are [17,18]

$$\Phi_{P,V}(x,\mu) = 6x(1-x)\left[1 + \sum_{n=1}^{\infty} a_n^{P,V}(\mu) C_n^{3/2}(2x-1)\right], \tag{28}$$

and twist-3 ones are [17,18]

$$\begin{aligned} &\Phi_p(x) = 1, \qquad \Phi_\sigma(x) = 6x(1-x), \\ &\Phi_v(x,\mu) = 3\left[2x - 1 + \sum_{n=1}^{\infty} a_n^{\perp,V}(\mu) P_{n+1}(2x-1)\right], \end{aligned} \tag{29}$$

where $C_n(x)$ and $P_n(x)$ are the Gegenbauer and Legendre polynomials, respectively. $a_n(\mu)$ are Gegenbauer moments that depend on the scale μ $(= 1$ GeV), and the values of Gegenbauer moments are taken from [22]

$$\begin{aligned} &a_1^\rho = 0, \qquad a_2^\rho = 0.15 \pm 0.07, \qquad a_1^{\perp\rho} = 0, \\ &a_2^{\perp\rho} = 0.14 \pm 0.06, \\ &a_1^\omega = 0, \qquad a_2^\omega = 0.15 \pm 0.07, \qquad a_1^{\perp\omega} = 0, \\ &a_2^{\perp\omega} = 0.14 \pm 0.06, \\ &a_1^\pi = 0, \qquad a_2^\pi = 0.25 \pm 0.15. \end{aligned} \tag{30}$$

The heavy-to-light form factors obtained from QCD sum rule calculations have the following values (at $k^2 = 0$) [22]:

$$\begin{aligned} &A_0^{B\rho}(0) = 0.303 \pm 0.029, \\ &A_0^{B\omega}(0) = 0.281 \pm 0.030, \\ &F_1^{B\pi}(0) = 0.25 \pm 0.03. \end{aligned} \tag{31}$$

The study of hadronic B decays favors a smaller first inverse moment λ_B [22], where λ_B is defined by $\int_0^1 \frac{d\xi}{\xi}\Phi_B(\xi) \equiv \frac{m_B}{\lambda_B}$ with $\Phi_B(\xi)$ being the LCDA of the B meson. We shall use $\lambda_B = 350 \pm 150$ MeV [17]. A fit to the $B \to VP$ and $B \to PV$ decays yields $\rho^{PV} \approx 0.87$, $\rho^{VP} \approx 1.07$, $\phi^{PV} \approx -30°$ and $\phi^{VP} \approx -70°$ [22]. For the estimate of theoretical uncertainties, we shall assign an error of ± 0.1 to $\rho^{PV(VP)}$ and $\pm 20°$ to $\phi^{PV(VP)}$ [22]. We find that the local integrated direct CP violation is more sensitive to $\phi^{PV(VP)}$ in practice.

B. Numerical results for CP violation

It is found that there is a maximum value for the differential CP violating parameter, when the low invariant mass of the $\pi^+\pi^-$ pair is near the vicinity of the ω resonance, 0.780–0.785 GeV. To be more specific, we display the differential CP asymmetries in Figs. 1(a) and (b) for some values of the CKM matrix elements and the divergence parameters. This behavior has been discussed in the naive factorization [14], QCD factorization [15] and perturbative QCD approaches [16], respectively. According to Eq. (17), we integrate A_{CP} over the low

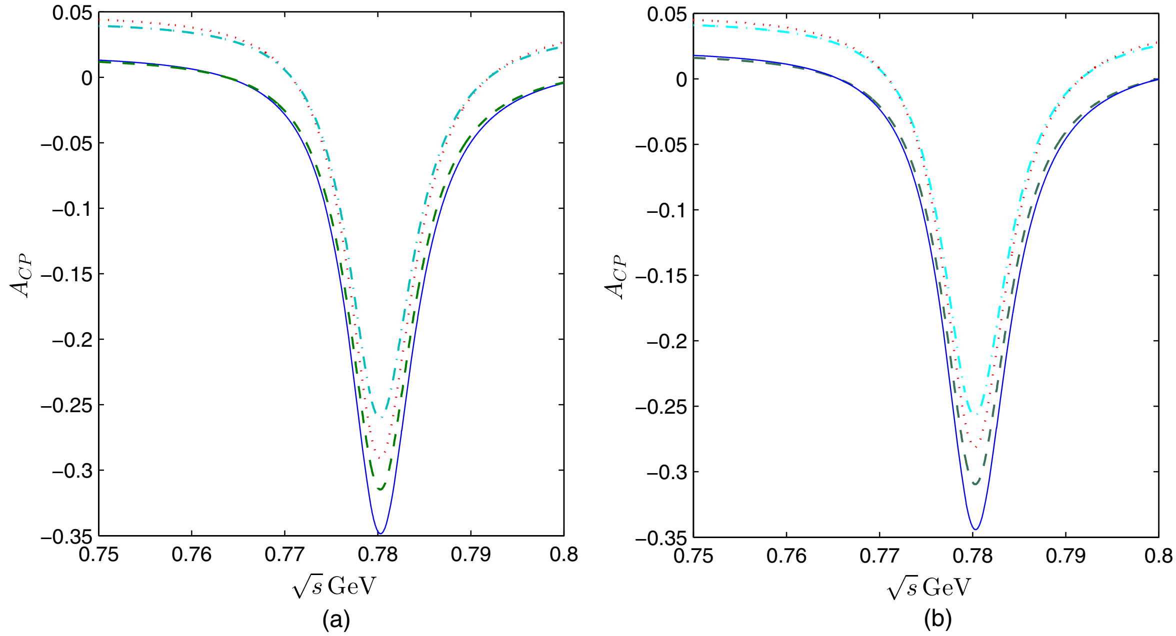

FIG. 1. The differential asymmetry, A_{CP}. (a) For $\rho^{PV} = 0.97$ and $\rho^{VP} = 1.17$: the solid (dot) line corresponds to $\phi^{PV} = -10°$ $(-50°)$ and $\phi^{VP} = -50°$ $(-90°)$ with minimum CKM matrix elements; the dashed (dot-dashed) line corresponds to $\phi^{PV} = -10°$ $(-50°)$ and $\phi^{VP} = -50°$ $(-90°)$ with maximum CKM matrix elements; (b) Same as (a) but for $\rho^{PV} = 0.77$ and $\rho^{VP} = 0.97$.

invariant mass of $\pi^+\pi^-$ $(\sqrt{s})$ and obtain the localized integrated asymmetries A^{Ω}_{CP}. Considering the significant region of ρ-ω mixing, we choose the integration interval of $\sqrt{s}$ to be from 0.750 to 0.800 GeV. In order to compare with the newest result of the LHCb experiments, we also calculate A^{Ω}_{CP} when $\sqrt{s}$ is in the low-mass region $(0.470 < \sqrt{s} < 0.770$ GeV) and the high-mass region $(0.770 < \sqrt{s} < 0.920$ GeV) near the ρ^0 resonance [8]. The numerical results are displayed in the Table I. We also display A^{Ω}_{CP} with and without ρ-ω mixing when $0.750 < \sqrt{s} < 0.800$ GeV in Table I.

Table I shows that the values of A^{Ω}_{CP} in our calculations vary from -0.0724 to -0.0389 in the variation ranges of the CKM matrix elements, $\phi^{PV,VP}$ and $\rho^{PV,VP}$ when $0.750 < \sqrt{s} < 0.800$ GeV. The localized integrated CP asymmetry obtained from experiments is -0.0294 ± 0.0285 when $0.750 < m(\pi^+\pi^-)_{\text{low}} < 0.800$ GeV. The values in our calculations agree with this experimental data. We stress that A^{Ω}_{CP} with ρ-ω mixing in this calculation is always negative and the sign of A^{Ω}_{CP} without ρ-ω mixing is always positive in this integration region. This indicates that ρ-ω mixing is vital for A^{Ω}_{CP} to be negative in this region.

According to the above discussions, we note that ρ-ω mixing changes the sign of A^{Ω}_{CP} from positive to negative in its significant region. From the plot of the differential CP violating parameter, we can see that the peak of the differential asymmetry A_{CP} involving ρ-ω mixing is on the right of 0.770 GeV [14–16]. Therefore, comparing with

TABLE I. The localized integrated asymmetries A^{Ω}_{CP} (in 10^{-2}) for $\rho^{PV} = 0.97(0.77)$ and $\rho^{VP} = 1.17(0.97)$. For each value of $\bar{\eta}$ and $\bar{\rho}$, the first and second lines correspond to A^{Ω}_{CP} with and without ρ-ω mixing, respectively, when $0.750 < \sqrt{s} < 0.800$ GeV, and the third and fourth lines correspond to the low-mass region $(0.470 < \sqrt{s} < 0.770$ GeV) and the high-mass region $(0.770 < \sqrt{s} < 0.920$ GeV) near the resonance mass, respectively. For other input parameters, we take their center values.

	$\phi^{VP} = -50°$ $\phi^{PV} = -10°$	$\phi^{VP} = -50°$ $\phi^{PV} = -50°$	$\phi^{VP} = -90°$ $\phi^{PV} = -10°$	$\phi^{VP} = -90°$ $\phi^{PV} = -50°$
$\bar{\eta} = 0.096$, $\bar{\rho} = 0.344$				
$0.750 < \sqrt{s} < 0.800$ GeV	$-7.24(-7.09)$	$-5.71(-5.89)$	$-5.70(-5.86)$	$-4.36(-4.78)$
	$4.33(4.57)$	$2.88(3.42)$	$3.34(3.73)$	$2.08(2.71)$
$0.470 < \sqrt{s} < 0.770$ GeV	$5.06(5.31)$	$3.44(4.04)$	$3.86(4.30)$	$2.47(3.17)$
$0.770 < \sqrt{s} < 0.920$ GeV	$-5.22(-5.21)$	$-3.89(-4.18)$	$-4.13(-4.33)$	$-2.98(-3.40)$
$\bar{\eta} = 0.139$, $\bar{\rho} = 0.366$				
$0.750 < \sqrt{s} < 0.800$ GeV	$-6.46(-6.33)$	$-5.10(-5.27)$	$-5.09(-5.23)$	$-3.89(-4.27)$
	$3.87(4.08)$	$2.57(3.06)$	$2.98(3.33)$	$1.87(2.42)$
$0.470 < \sqrt{s} < 0.770$ GeV	$4.52(4.75)$	$3.06(3.61)$	$3.45(3.84)$	$2.20(2.83)$
$0.770 < \sqrt{s} < 0.920$ GeV	$-4.66(-4.66)$	$-3.48(-3.73)$	$-3.69(3.86)$	$-2.67(-3.03)$

TABLE II. The localized integrated asymmetries A_{CP}^{Ω} (in 10^{-2}) obtained in the QCD factorization and naive factorization approaches compared with the experimental data.

$\sqrt{s}$ (GeV)	$0.750 < \sqrt{s} < 0.800$	$0.470 < \sqrt{s} < 0.770$	$0.770 < \sqrt{s} < 0.920$
Experimental data	(−5.79, −0.09)	(3.37, 6.79)	(−4.58, −0.54)
QCD factorizaion	(−7.24, −3.89)	(2.20, 5.31)	(−5.22, −3.03)
Naive factorization	(−7.52, −2.90)	(−0.94, 3.53)	(-4.08, 0.46)(−4.08, 0.46)

A_{CP}^{Ω} in the range $0.470 < \sqrt{s} < 0.770$ GeV, the localized integrated CP asymmetries move toward the negative direction when $0.770 < \sqrt{s} < 0.920$ GeV due to ρ-ω mixing. This behavior contributes to the sign change around the ρ resonance, as in the naive factorization approach [9]. In the QCD factorization approach, A_{CP}^{Ω} in regions $0.470 < m(\pi^+\pi^-)_{\mathrm{low}} < 0.770$ GeV and $0.770 < m(\pi^+\pi^-)_{\mathrm{low}} < 0.920$ GeV are from 0.0220 to 0.0531 and from −0.0522 to −0.0303, respectively. The experimental data in the regions $0.470 < m(\pi^+\pi^-)_{\mathrm{low}} < 0.770$ GeV and $0.770 < m(\pi^+\pi^-)_{\mathrm{low}} < 0.920$ GeV are 0.0508 ± 0.0171 and -0.0256 ± 0.0202, respectively. We can see our results agree with experiments and it is clear that ρ-ω mixing does contribute to the sign change in those two regions.

In Table II, we compare the localized integrated direct CP violation involving ρ-ω mixing in the naive factorization [9] and QCD factorization approaches. The localized integrated direct CP violations in the naive factorization are (−0.0724, −0.0389), (0.0220, 0.0531), and (−0.0522, −0.0303) corresponding to $0.750 < \sqrt{s} < 0.800$ GeV, $0.470 < \sqrt{s} < 0.770$ GeV, and $0.770 < \sqrt{s} < 0.920$ GeV, respectively. One can see the results in the QCD factorization approach agree with the experimental data and the ranges of their values are smaller. In both the naive and the QCD factorization approaches ρ-ω mixing contributes to the sign change of CP asymmetry between the regions $0.470 < m(\pi^+\pi^-)_{\mathrm{low}} < 0.770$ GeV and $0.770 < m(\pi^+\pi^-)_{\mathrm{low}} < 0.920$ GeV.

V. CONCLUSION AND DISCUSSION

In this work, we have studied the localized integrated CP asymmetry for the decays $B^{\pm} \to \rho^0(\omega)\pi^{\pm} \to \pi^+\pi^-\pi^{\pm}$ with the inclusion of ρ-ω mixing and the sign change caused by ρ-ω mixing in the QCD factorization approach which is expected to be a reliable approach in the heavy-quark limit. The results are consistent with the experimental data and are more accurate than those in the naive factorization approach which were obtained in our previous work.

The value of A_{CP}^{Ω} in the region $0.750 < m(\pi^+\pi^-)_{\mathrm{low}} < 0.800$ GeV varies from −0.0724 to −0.0389. This result, especially the sign, agrees with the experimental data. We cannot obtain the right CP asymmetry parameter without ρ-ω mixing. In the regions $0.470 < m(\pi^+\pi^-)_{\mathrm{low}} < 0.770$ GeV and $0.770 < m(\pi^+\pi^-)_{\mathrm{low}} < 0.920$ GeV, A_{CP}^{Ω} are from 0.0220 to 0.0531 and from −0.0522 to −0.0303, respectively, and agree with the experimental data. This explains the sign change of CP asymmetry between the regions $0.470 < m(\pi^+\pi^-)_{\mathrm{low}} < 0.770$ GeV and $0.770 < m(\pi^+\pi^-)_{\mathrm{low}} < 0.920$ GeV. We conclude that ρ-ω mixing contributes to the sign change of the CP violating asymmetry around the $\rho^0(770)$ peak of $m(\pi^+\pi^-)_{\mathrm{low}}$ and should be taken into account in the calculations of CP violation.

In the calculations of CP asymmetry for the decays $B^{\pm} \to \rho^0(\omega)\pi^{\pm} \to \pi^+\pi^-\pi^{\pm}$, the large strong phase mainly comes from ρ-ω mixing in the naive factorization approach. On the other hand, in the QCD factorization scheme, $\alpha_s(m_b)$ corrections at the leading order of $1/m_b$ are included and the strong phase can also be generated dynamically. Since the way to introduce the strong phase is different in these two approaches, studying the direct CP violation, especially the localized direct CP violation, could be a good way to check their validities. As we expected, the QCD factorization approach is more reliable and the results in this approach are more accurate. In the QCD factorization framework, there is cancellation of the scale and renormalization scheme dependence between the Wilson coefficients and the hadronic matrix elements. However, there still remain some uncertainties in this calculations. The QCD factorization suffers from endpoint singularities which cause the main uncertainties. The CP violating asymmetry depends on the unknown parameters ($\rho^{PV(VP)}$ and $\phi^{PV(VP)}$) which are associated with such singularities [17,18]. These uncertainties can be reduced if we select the divergence parameters appropriately [22]. One requires more accurate experimental data to determine these divergence parameters. The further calculation of the amplitude for $B^{\pm} \to \rho^0(\omega)\pi^{\pm}$ at next-to-next-to leading order in the QCD factorization approach introduces new rescattering phases that modify the leading-order result and the direct CP asymmetry could be calculated more accurately [30–33]. Besides, it is now apparent that the CKM matrix is the primary source of direct CP violation in flavor changing processes in B decays and not well determined. Therefore, the CKM matrix parameters can also bring some uncertainties.

ACKNOWLEDGMENTS

This work was supported in part by National Natural Science Foundation of China (Project Nos. 11175020, 11275025, 11447021, and 11575023).

[1] J. H. Christenson, J. W. Cronin, V. L. Fitch, and R. Turlay, Phys. Rev. Lett. **13**, 138 (1964).
[2] N. Cabibbo, Phys. Rev. Lett. **10**, 531 (1963).
[3] M. Kobayashi and T. Maskawa, Prog. Theor. Phys. **49**, 652 (1973).
[4] A. B. Carter and A. Sanda, Phys. Rev. D **23**, 1567 (1981).
[5] I. I. Bigi and A. Sanda, Nucl. Phys. **B193**, 85 (1981).
[6] J. M. de Miranda (LHCb Collaboration), *Proceedings of CKM 2012, the 7th International Workshop on the CKM unitarity, University of Cincinnati, Cincinnati, 2012*; arXiv:1301.0283.
[7] R. Aaij *et al.* (LHCb Collaboration), Phys. Rev. Lett. **112**, 011801 (2014).
[8] R. Aaij *et al.* (LHCb Collaboration), Phys. Rev. D **90**, 112004 (2014).
[9] C. Wang, Z.-H. Zhang, Z.-Y. Wang, and X.-H. Guo, Eur. Phys. J. C **75**, 536 (2015).
[10] R. Enomoto and M. Tanabashia, Phys. Lett. B **386**, 413 (1996).
[11] S. Gardner, H. B. O'Connell, and A. W. Thomas, Phys. Rev. Lett. **80**, 1834 (1998).
[12] X.-H. Guo and A. W. Thomas, Phys. Rev. D **58**, 096013 (1998); **61**, 116009 (2000).
[13] C. Wang, X.-H. Guo, Y. Liu, and R.-C. Li, Eur. Phys. J. C **74**, 3140 (2014).
[14] X.-H. Guo, O. Leitner, and A. W. Thomas, Phys. Rev. D **63**, 056012 (2001).
[15] O. Leitner, X.-H. Guo, and A. W. Thomas, J. Phys. G **31**, 199 (2005).
[16] G. Lü, B. H. Yuan, and K. W. Wei, Phys. Rev. D **83**, 014002 (2011).
[17] M. Beneke and M. Neubert, Nucl. Phys. **B675**, 333 (2003).
[18] M. Beneke, G. Buchalla, M. Neubert, and C. T. Sachrajda, Nucl. Phys. **B606**, 245 (2001).
[19] J. D. Bjorken, Nucl. Phys. B, Proc. Suppl. **11**, 325 (1989).
[20] M. J. Dugan and B. Grinstein, Phys. Lett. B **255**, 583 (1991).
[21] C. W. Bauer, I. Z. Rothstein, and I. W. Stewart, Phys. Rev. D **74**, 034010 (2006).
[22] H.-Y. Cheng and C.-K. Chua, Phys. Rev. D **80**, 114008 (2009).
[23] Z.-H. Zhang, X.-H. Guo, and Y.-D. Yang, Phys. Rev. D **87**, 076007 (2013).
[24] Z.-H. Zhang, X.-H. Guo, and Y.-D. Yang, arXiv:1308.5242.
[25] I. Bediaga, G. Guerrer, and J. M. de Miranda, Phys. Rev. D **76**, 073011 (2007).
[26] H. B. O'Connell, A. W. Thomas, and A. G. Williams, Nucl. Phys. **A623**, 559 (1997); K. Maltman, H. B. O'Connell, and A. G. Williams, Phys. Lett. B **376**, 19 (1996).
[27] S. Gardner and H. B. O'Connell, Phys. Rev. D **57**, 2716 (1998).
[28] M. Wirbel, B. Stech, and M. Bauer, Z. Phys. C **29**, 637 (1985).
[29] K. A. Olive *et al.* (PDG Collaboration), Chin. Phys. C **38**, 090001 (2014).
[30] G. Bell and V. Pilipp, Phys. Rev. D **80**, 054024 (2009).
[31] M. Beneke, T. Huber, and X.-Q. Li, Nucl. Phys. **B832**, 109 (2010).
[32] G. Bell, *Proc. Sci.*, RADCOR2009 (2010) 028.
[33] G. Bell, M. Beneke, T. Huber, and X.-Q. Li, Phys. Lett. B **750**, 348 (2015).